*Work supported in part by a City University of New York summer research grant.

[1]B. G. Peterson, in *Alpha-, Beta-, and Gamma-Ray Spectroscopy*, edited by K. Siegbahn (North-Holland Publishing Company, Amsterdam, The Netherlands, 1966), Vol. 2, p. 1574.

[2]D. Berenyi, Rev. Mod. Phys. 40, 390 (1968).

[3]P. C. Martin and R. J. Glauber, Phys. Rev. 109, 1307 (1958).

[4]H. Lancman and J. M. Lebowitz, Phys. Rev. 188, 1683 (1969).

[5]H. Lancman and J. M. Lebowitz, Bull. Am. Phys. Soc. 15, 23 (1970).

[6]J. Rapaport, Nucl. Data B3(No. 3, 4), 126 (1970).

[7]C. H. Johnson, C. C. Trail, and A. Galonsky, Phys. Rev. 136, B1719 (1964).

[8]R. G. Jung and M. L. Pool, Bull. Am. Phys. Soc. 1, 172 (1956).

PHYSICAL REVIEW C VOLUME 3, NUMBER 1 JANUARY 1971

Recoil-Distance Lifetime Measurements for States in P^{30}†

S. H. Henson, S. Cochavi, M. Marmor, and D. B. Fossan
State University of New York, Stony Brook, New York 11790
(Received 26 June 1970)

The recoil-distance method has been used with the $Al^{27}(\alpha, n)P^{30}$ reaction to measure the lifetimes of the 1.453- and 1.974-MeV levels in P^{30}. A mean lifetime of $\tau = 9.2 \pm 0.5$ psec was obtained for the 2^+ 1.453-MeV level and $\tau = 6.8 \pm 0.4$ psec was obtained for the 3^+ 1.974-MeV level. A Ge(Li) γ spectrum was measured in coincidence with neutrons to identify the P^{30} transitions. Comparisons of the resulting reduced transition probabilities with shell-model calculations have been made.

I. INTRODUCTION

The self-conjugate nucleus P^{30} has been studied extensively with the $S^{32}(d, \alpha)P^{30}$ and $Si^{29}(p, \gamma)P^{30}$ reactions.[1-3] Endt and Paris,[1] using the former reaction, located the energies of 30 excited states in P^{30} below 5.8 MeV. Van der Leun and Endt[2,3] observed the operation of $E1$ isospin selection rules for self-conjugate nuclei with the $Si^{29}(p,\gamma)P^{30}$ reaction. Additional $Si^{29}(p, \gamma)P^{30}$ studies were done by Baart, Green, and Willmott,[4] Moore,[5] and Harris, Hyder, and Walinga.[6]

Angular-correlation measurements have recently been performed by Vermette *et al.*[7] using the $Si^{28}(He^3, p\gamma)P^{30}$ reaction. Information on spins, mixing ratios, and branching ratios were obtained for 16 levels in P^{30} below 5-MeV excitation.

Several attempts have been made to theoretically interpret the experimental information on P^{30}. Despite the success of the strong-coupling collective model in this region, a rotational interpretation has not been staisfactory. Vibration and intermediate-coupling approaches were only partially successful. Glaudemans, Wiechers, and Brussard[8] (GWB) made shell-model calculations for P^{30} assuming an inert Si^{28} core and two-particle interactions for the outer nucleons in the $2s_{1/2}$ and $1d_{3/2}$ shells. Although a number of the level energies and spins were successfully fit, several of the observed levels could not be explained by means of this truncated shell-model picture. A large shell-model calculation is at present underway for the $A = 30$ region.[9] It is hoped that such a calculation will form a more complete theory for P^{30} and the neighboring nuclei, as has been the case for lighter nuclei.

Nuclear-structure information can often be extracted from the study of electromagnetic interactions in nuclei; γ-ray transition probabilities between states i and f are proportional to the reduced matrix element, $\langle \psi_f \| \theta_l \| \psi_i \rangle$, where ψ_f and ψ_i are nuclear wave functions and θ_l is the electromagnetic operator of order l. An experimental determination of such matrix elements allows a sensitive test of nuclear wave functions and thus the nuclear structure. The purpose of the present experiment is to seek more knowledge concerning the structure of P^{30} by measuring various nuclear lifetimes in this nucleus.

In this experiment the recoil distance or so called plunger technique will be employed in the lifetime range of 10^{-12} to 10^{-10} psec; the plunger technique is the most accurate technique for measuring lifetimes in this timing range. Delayed-coincidence timing is only applicable for lifetimes greater than about 10^{-10} sec, and the Doppler-shift-attenuation method (DSAM) can best be used for lifetimes in the range of 10^{-15} to 10^{-12} sec. The uncertainty in the energy loss of charged particles in matter limits the accuracy of the DSAM for lifetimes greater than a few psec.

The nucleus P^{30} is a self-conjugate nucleus where $\Delta T = 0$ $M1$ transitions are strongly hindered. Several γ transitions in P^{30} expected to be predominantly $M1$ have energies that would make the lifetimes of the initial state fall into the plunger range. One of these was measured with the plunger, as well as several $E2$ transitions. Preliminary results for these measurements have been reported.[10]

Kennedy, Youngblood, and Blaugrund,[11] using the DSAM, have measured the mean lifetime of the first excited 0^+ state as $\tau = 0.155 \pm 0.030$ psec. Concurrently with our experiment, electromagnetic studies by the DSAM were being performed on other P^{30} states. Preliminary reports[12,13] from these experiments are available. These DSAM measurements and the present plunger-technique measurements combine into a thorough electromagnetic study of the nuclear structure of P^{30}.

II. EXPERIMENTAL TECHNIQUE

A. Plunger Measurements

The excited states of P^{30} are populated for these measurements with the reaction $Al^{27}(\alpha, n)P^{30}$; the ground-state Q value is $Q = -2.65$ MeV. The P^{30} excited states relevant to this experiment are illustrated in Fig. 1. For suitable α energies, the kinematics of this reaction limit the excited P^{30} recoils to a narrow forward cone with large recoil velocities.

The plunger technique recently reviewed by Jones *et al.*[14] is illustrated in Fig. 2. Details of the present plunger apparatus are similar to those described in Ref. 14. The excited P^{30} nuclei, which are produced by the α beam in a 100-μg/cm^2 Al target, recoil freely into vacuum with a component of velocity, v, in the beam direction. The Al target was evaporated on the back side of a 2-mg/cm^2 gold foil for strength. The position of this target along the beam direction was precisely defined by radially stretching the target foil with a V-groove, O-ring arrangement; the α beam was collimated to a spot diameter of 3 mm. A thick gold stopper (plunger) as shown, was designed to be positioned precisely at variable distances D from the target. The excited P^{30} nuclei that γ decay while recoiling in the vacuum exhibit Doppler-shifted γ rays; those excited nuclei that survive for a time greater than D/v are stopped by the plunger and thus emit unshifted γ rays. These two related γ-ray peaks can often be resolved in the energy spectrum of a Ge(Li) detector. For 0° detection, the energy separation of the two peaks corresponding to a γ ray of energy E_0 is

$$\Delta E = E_0(v/c). \tag{1}$$

The intensities of the Doppler-shifted peak I_s and the unshifted peak I_0 are

$$I_s = N(1 - e^{-D/v\tau}), \quad I_0 = Ne^{-D/v\tau}, \tag{2}$$

where N is the total number of γ rays and τ the mean lifetime of the excited state. A measurement of the ratio $R = I_0/(I_0 + I_s)$ as a function of D, which is given by

$$R = e^{-D/v\tau}, \tag{3}$$

yields the mean life τ, as v can be determined from the γ-ray energy spectrum using Eq. (1) or from the reaction kinematics.

For most measurements, there is not a unique value of the recoil velocity v but a finite spread of recoil velocities due to target thickness and variation in recoil angle. This spread in velocities re-

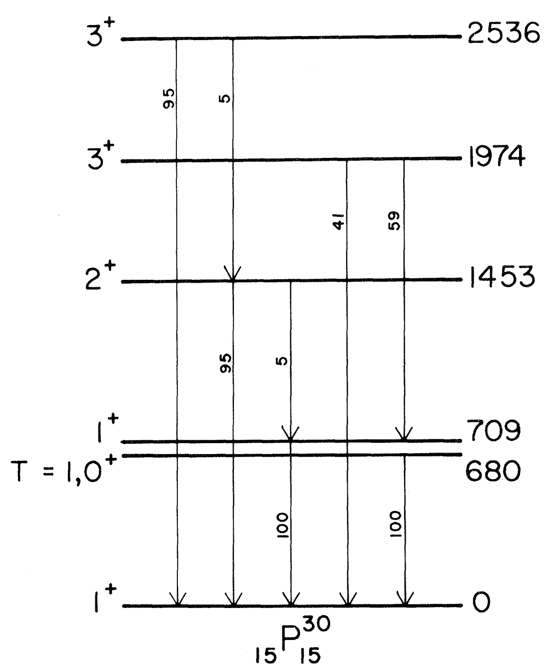

FIG. 1. Prominent γ-ray transitions observed in P^{30}. The level scheme, spin-parity parameters, and branching ratios are consistent with those listed by Vermette *et al.* in Ref. 7.

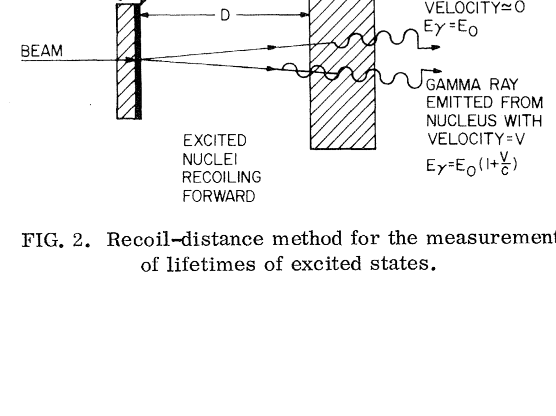

FIG. 2. Recoil-distance method for the measurement of lifetimes of excited states.

sults in a broadened shifted peak. The ratio R for a spread of recoil velocities becomes

$$R=\sum_n A_n e^{-D/v_n\tau}\,, \tag{4}$$

where v_n represents a value of the component of recoil velocity and A_n the fraction ($\sum_n A_n=1$) of all recoils having v_n. The A_n are determined from the number of counts in the nth energy channel of the Doppler-shifted peak and the v_n from Eq. (1); appropriate account has to be taken for the energy resolution of the γ-ray detection system.

Several small corrections and uncertainty considerations have to be applied to the above treatment.[14] These include effects from solid-angle differences, detector geometry, efficiency variations, and small uncertainties in the distance D. The detailed consideration of these effects for the present data will be discussed later.

The γ-ray spectra in the present measurements were measured with a 30-cc Ge(Li) detector which was positioned at 0° to the beam direction and 7 cm from the target. Pole-zero and dc-restoration electronics were employed for high counting rates. The energy resolution of the system was 3.5 keV at 1.33 MeV. A 1024-channel pulse-height analyzer was used to record the γ spectra in conjunction with a biased amplifier.

An excitation study was made of the $Al^{27}(\alpha,n)P^{30}$ reaction from 7- to 15-MeV α energy by observing the Ge(Li) singles γ spectra. At small plunger distances D, Doppler-shifted peaks were observed simultaneously with unshifted peaks for γ rays of energy 0.709, 1.265, 1.453, and 1.974 MeV. These doublet peaks indicate lifetimes which can be measured by the plunger technique. As seen from energy considerations in Fig. 1, the 0.709-MeV γ ray is consistent with the decay of the second 1^+ level in P^{30}, the 1.453-MeV γ ray with the first 2^+ state, and the 1.265- and 1.974-MeV γ rays with the 3^+ level at 1.974 MeV. An α energy of $E_\alpha=8.7$ MeV was chosen for optimum yield to the 1.453- and 1.974-MeV states. Since the 0.709-MeV state has been measured with fair accuracy by a gas DSAM,[12] since the energy resolution of the detector was only marginal for this low energy, and since the above α energy has unfavorable recoil kinematics for this state, it was decided to concentrate the present experiment on the 1.453- and 1.974-MeV states.

For the plunger lifetime measurements, singles Ge(Li) spectra were taken for several plunger distances D which cover the decay curves. A minimum distance of about 0.2 mil could be achieved with the plunger apparatus. The duration of the γ measurements was increased for larger D to accumulate sufficient statistics in the ratio R. Measurements at small and large D were alternated. Spectra with good statistics were taken at a distance $D \gg v\tau$ at the beginning and end of the plunger experiments to determine any background in the ratio R.

B. Neutron-γ-Coincidence Measurements

In order to insure that the singles γ-ray spectra

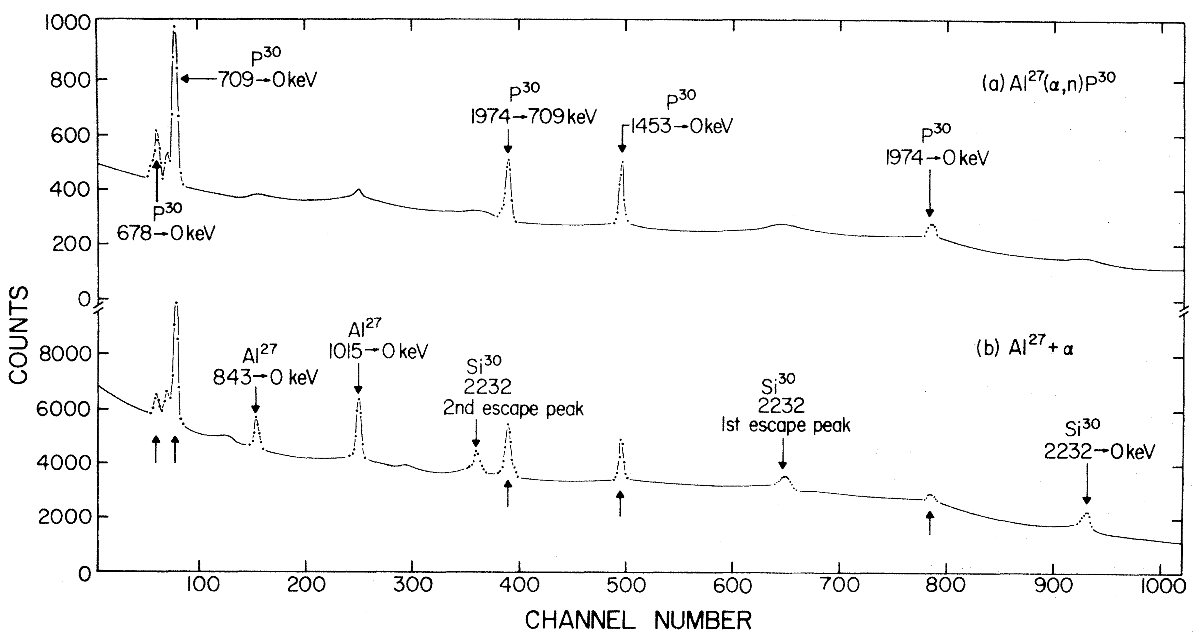

FIG. 3. (a) Ge(Li) γ-ray spectrum observed at 90° in coincidence with neutrons at 0° for $E_\alpha=8.7$ MeV from the $Al^{27}(\alpha,n)P^{30}$ reaction. Randoms have not been subtracted. (b) γ-ray singles spectrum for $Al^{27}+\alpha$.

analyzed in this experiment are definitely associated with the $Al^{27}(\alpha, n\gamma)P^{30}$ reaction, a neutron-γ coincidence measurement was performed. A thick Al target of about 1 mg/cm^2 was bombarded with 8.7-MeV α particles; the Ge(Li) γ spectrum at 90° was recorded in coincidence with 0° neutrons detected in an NE213 liquid scintillator that was coupled to an RCA 8575 photomultiplier tube. To avoid γ-γ coincidences, the γ pulses from the NE213 scintillator were discriminated against by pulse-shape analysis.[15] The neutron-induced recoil-proton pulses exhibit a larger slow-decay component than the γ-produced Compton-electron pulses. These different pulse shapes were identified by measuring the time delay between the fast component observed at the anode and the bipolar crossover of the corresponding integrated dynode signal. These time delays for the neutron and γ-ray pulses as measured by a time-to-amplitude converter (TAC) showed a difference of about 15 nsec. A single-channel analyzer was used at the output of the TAC to select the neutrons for the coincidence requirement.

The resulting Ge(Li) γ spectrum in coincidence with neutrons is shown in Fig. 3(a). The prominent peaks observed at 0.678, 0.709, 1.265, 1.453, and 1.974 MeV are associated with the P^{30} transitions indicated on the figure. Random events have not been subtracted from this spectrum.

The corresponding singles γ spectrum is shown in Fig. 3(b). In addition to the P^{30} γ rays, the 2.232-MeV γ ray and its escape peaks are identified with the first excited state of Si^{30} produced by the $Al^{27}(\alpha, p)Si^{30}$ reaction and the 0.843- and 1.015-MeV γ rays result from the $Al^{27}(\alpha, \alpha')Al^{27}$ reaction. As will be discussed later, the 1.265-MeV P^{30} γ peak contains an unresolved shoulder which is due to the 1.264-MeV γ ray from Si^{30}. The 1.453- and 1.974-MeV γ peaks of P^{30} are isolated from contaminant peaks and, therefore, can be easily analyzed from singles measurements.

III. EXPERIMENTAL RESULTS

Representative γ spectra for the plunger measurement of the P^{30} 1.453 → 0 transition are displayed in Fig. 4. The spectra of the unshifted stopped peak I_0 and the Doppler-shifted peak I_s are shown for three plunger distances D; it can be seen that the relative intensity of I_0 to I_s decreases as D increases. The intensities I_0 and I_s for the different D were extracted with a fit to measured peak shapes and the background. The ratio $R = I_0/(I_0 + I_s)$ for the 1.453-MeV γ ray is plotted as a function of D in Fig. 5. Uncertainties due to statistics and distance measurements are indicated by error boxes. The distance uncertainty was estimated from reproducibility measurements as ±0.05 mil. Only relative distances were measured; the zero of distance was assigned in Fig. 5 to the point where the ratio R extrapolated linearly to unity.

The data in Fig. 5 were least-squares-fitted to Eq. (3) for a recoil velocity that corresponds to the centroid of the Doppler-shifted peak. On the semilog plot of Fig. 5 this fit appears as the dashed straight line. From Eq. (1) an energy difference of $\Delta E = 11.5$ keV between this centroid and that of the unshifted peak implies a $v/c = 0.794\%$. The resulting mean lifetime for the 1.453-MeV state of P^{30} is 8.4 psec.

To include the effect of a spread in recoil velocities which is manifest in the broadened shifted peak, a least-squares fit of the data was made to Eq. (4). The peaks were assumed to be Gaussian so that the width ω of the velocity distribution is given by $\omega = (\omega_s{}^2 - \omega_0{}^2)^{1/2}$, where ω_s is the width of the shifted peak and ω_0 is the instrumental resolution width, namely, the width of the unshifted peak. The Doppler-shifted peak, which is divided up into n energy channels, was converted to the velocity distribution by adjusting for the resolution width

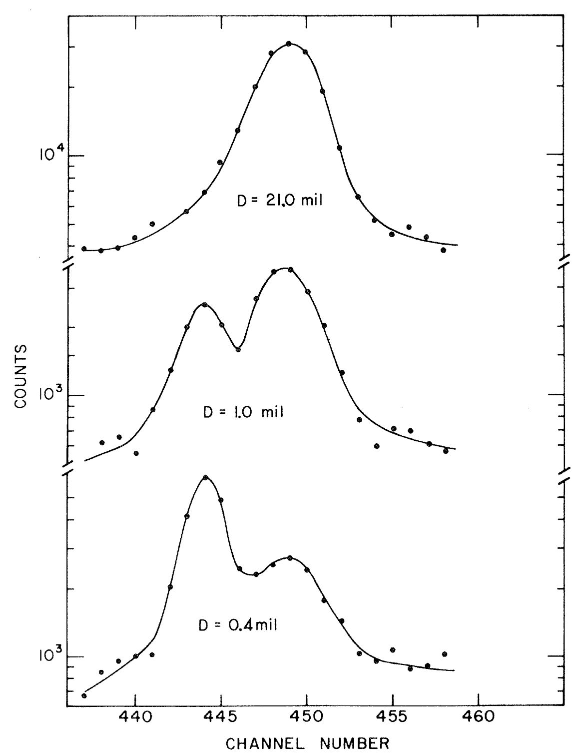

FIG. 4. The P^{30} 1.453-MeV → 0 energy peak viewed at 0° to the α beam in the $Al^{27}(\alpha, n)P^{30}$ reaction at $E_\alpha = 8.7$ MeV. The presence of two γ-ray peaks with average energies E_0 and $E_0(1 + v/c)$ is evident as is the dependence of the relative intensities of these two peaks on the plunger displacement D. The energy dispersion is 2.129 keV/channel. (1 mil = 25.4 μ.)

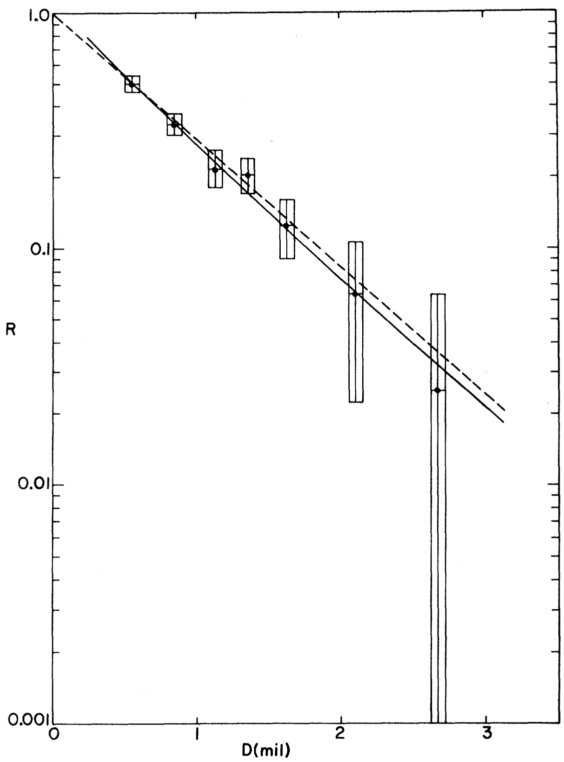

FIG. 5. Decay curves for the 1.453-MeV → 0 transition. The dashed straight line represents the least-squares fit using the approximation that the recoil velocity corresponds to the centroid of the Doppler-shifted peak. A least-squares fit which includes the effect of the spread in recoil velocities is represented by the solid curved line.

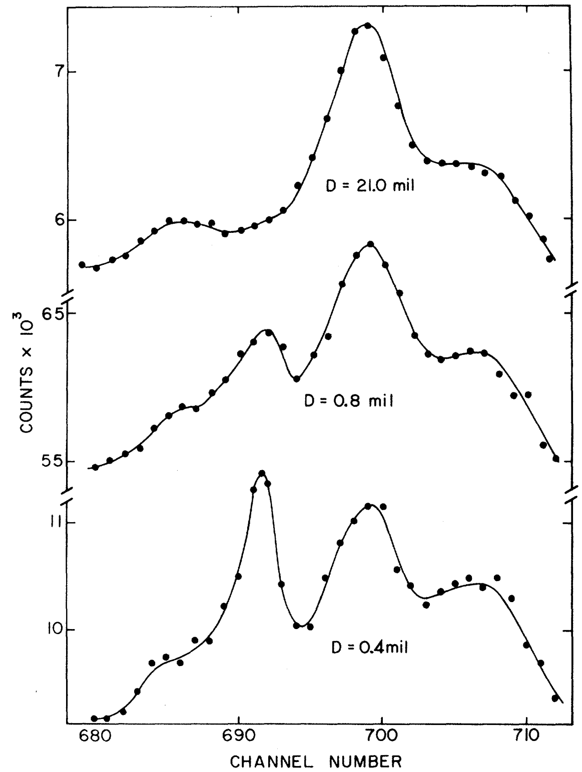

FIG. 6. Representative γ spectra for the shifted and unshifted peaks of the P^{30} 1.974-MeV → 0 transition for three distances. The energy dispersion is 2.129 keV/channel. (1 mil = 25.4 μ.)

in this manner. The A_n which represent the fraction of counts in the nth channel to the total number of counts in the shifted peak were determined from the resulting velocity distribution. The velocities v_n associated with the nth channel were obtained from Eq. (1). To fit the data to Eq. (4), the absolute distances D are required. Since only relative D were measured, the fit was made as a function of both the zero of distance and τ. The resulting best fit is shown by the solid curved line in Fig. 5; the corresponding mean lifetime for the 1.453-MeV state is $\tau = 9.4$ psec. As several γ rays were measured at the same time, the choice of the zero of distance must be the same for each and, therefore, is well defined. A lifetime comparison is made in Table I which shows results for the assumption of the centroid velocity, results for the proper velocity distribution, and final corrected results which include several small additional corrections. These additional corrections, mentioned earlier, will be discussed for all of the results at the end of this section.

Representative γ spectra for the shifted and unshifted peaks of the P^{30} 1.974 → 0 transition are shown in Fig. 6 for three distances. The data for this transition were analyzed in a manner similar to that discussed for the 1.453-MeV γ ray. Special care had to be applied in extracting the intensities I_0 and I_s for the 1.974-MeV γ ray because of the broad peak at about channel 707, which is the Compton edge of the Si^{30} 2.232-MeV γ ray, and because of the small unassigned peak at channel 685.

TABLE I. Results of data analysis.

Transition (MeV)	Linear fit	Velocity distribution fit	Final corrected value (psec)
1.453 → 0	8.4 psec	9.4 psec	9.2 ± 0.5 psec
1.974 → 0	7.0 psec	7.0 psec	6.8 ± 0.4 psec
1.974 → 0.709	5.7	6.4	

The ratios R extracted from the data for this ground-state transition are plotted in the upper portion of Fig. 7. The fit to Eq. (3) for the centroid velocity which is displayed by the dashed straight line yields a mean lifetime of $\tau = 7.0$ psec. With the velocity distribution measured from the shifted peak, a fit to Eq. (4) also gives a mean lifetime of $\tau = 7.0$ psec; this fit is shown in the upper portion of Fig. 7 by the solid curved line.

The $1.974 \rightarrow 0.709$ γ branch gives an additional measurement of the lifetime of the P^{30} 1.974-MeV state. As mentioned earlier, the shifted peak for this 1.265-MeV γ ray contains an unresolved contaminant from the 1.264-MeV $2^+ \rightarrow 2^+$ transition of Si^{30}. Since the second 2^+ state in Si^{30} has a relatively short mean lifetime[16] ($\tau = 0.15 \pm 0.02$ psec) this contaminant γ ray should not effect this P^{30} lifetime measurement as long as the ratio R is not forced through unity at $D = 0$. The extracted ratios R for this P^{30} 1.265-MeV γ ray are plotted as a function of D in the lower portion of Fig. 7. As is seen in this figure, the extrapolated ratio at $D = 0$ is only

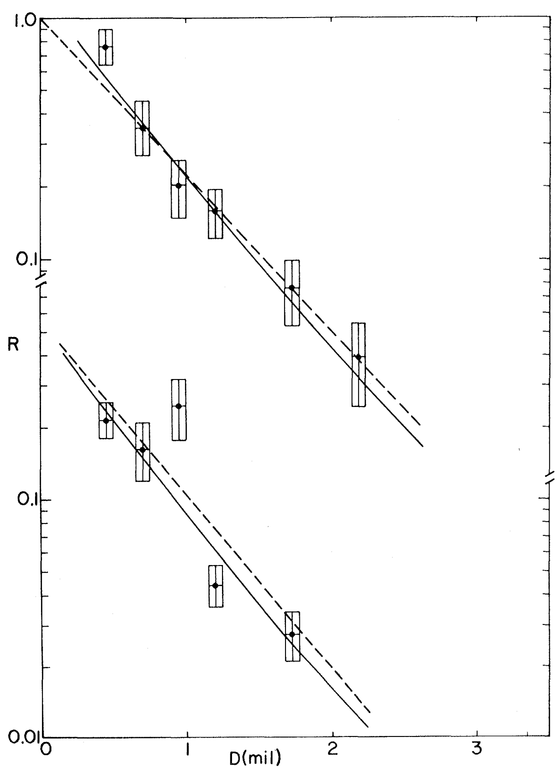

FIG. 7. Decay curves for the 1.974-MeV$\rightarrow$0 transition are shown in the upper portion of the figure and decay curves for the $1.974 \rightarrow 0.709$-MeV transition in the lower portion. Dashed straight lines represent least-squares fits using the approximation that the recoil velocity corresponds to the centroid of the Doppler-shifted peak; solid curved lines represent fits which include the effect of the spread in recoil velocities.

$R \sim 0.5$. The mean lifetimes obtained, as discussed above from fits to Eqs. (3) and (4) are 5.7 and 6.4 psec, respectively; these fits are also shown in Fig. 7 with the same notation. A comparison of the lifetime results for the P^{30} 1.974-MeV state for both γ transitions is also given in Table I.

Several small corrections as discussed in detail by Jones *et al.*[14] have to be applied to these lifetimes in order to obtain the final results. The solid angle subtended by the γ detector is larger for a recoiling nucleus as compared with a stopped nucleus. The correction for this solid-angle effect is opposite to the small correction of efficiency due to the energy difference between the shifted and unshifted peaks. A correction must also be made in the measurement of the velocity distribution for the finite geometry of the γ detector. The sum of these corrections have been applied to the results obtained by fitting to Eq. (4) for the appropriate velocity distributions. This leads to a final value of $\tau = 9.2 \pm 0.5$ psec for the 1.453-MeV state in P^{30} and to $\tau = 6.8 \pm 0.4$ psec for the 1.974-MeV state as listed in Table I. The uncertainties were estimated from statistics, distance variations, and the quality of the fits.

IV. DISCUSSION

In the present experiment the plunger technique yielded mean lifetimes of $\tau = 9.2 \pm 0.5$ psec for the P^{30} 2^+ level at 1.453 MeV and $\tau = 6.8 \pm 0.4$ psec for the P^{30} 3^+ level at 1.974 MeV. Preliminary DSAM limits[12] of $\tau = 8 \pm 5$ psec and $\tau > 8$ psec are roughly consistent with these results for the 1.453- and 1.974-MeV levels, respectively, while other preliminary DSAM results[13] are not.

The results of the 1.453-MeV level imply reduced transition probabilities of $B(M1) = 1.4 \times 10^{-3} \mu_N{}^2$ and $B(E2) = 0.45\ e^2\mathrm{F}^4$ for the $(2^+ \rightarrow 1^+)$ ground-state transition using the previously measured[6] mixing ratio. The lifetime of the 1.974-MeV level along with the known branching ratio[7] yields a $B(E2) = 1.7\ e^2\mathrm{F}^4$ for the $(3^+ \rightarrow 1^+)$ ground-state transition and a $B(E2) = 22\ e^2\mathrm{F}^4$ for the 1.265-MeV $(3^+ \rightarrow 1^+)$ transition to the 0.709-MeV level. The reduced transition probabilities determined by the measurements of the present experiment are listed in Table II.

In comparison with single-particle estimates, these results show an $M1$ hinderance of 1000 and an $E2$ strength of 0.07 Weisskopf units (W.u.) for the 1.453-MeV transitions. For the 1.974- and 1.265-MeV transitions, the $E2$ strengths are 3.9 and 0.29 W.u., respectively. The large $M1$ hinderance is expected for $\Delta T = 0$ transitions in self-conjugate nuclei.[17]

As mentioned in the Introduction, no theoretical study to date has been successful in explaining the observed properties of P^{30}. The large shell-model calculation[9] presently being carried out is expected to yield a considerable improvement in the theoretical basis for this nucleus. The observed electromagnetic transition probabilities in P^{30} form a sensitive test of the wave functions generated in this theory. At the conclusion of the above theoretical study, a complete comparison of all of the experimentally observed properties near $A=30$ with theoretical predictions will measure the extent of the improved theoretical understanding.

For the present, the transition probabilities determined in this experiment will be compared with matrix elements calculated for approximate wave functions, namely those suggested by GWB[8] for a trucated $(2s_{1/2}\text{-}1d_{3/2})$ shell-model space. In this simplified theory, an inert Si^{28} core closing the $1d_{5/2}$ shell was assumed, and two-particle interactions were included for only the outer two nucleons in the $2s_{1/2}$ and $1d_{3/2}$ shells. The wave functions from this truncated space should represent a significant portion of the actual wave functions for a number of the levels in P^{30}.

The ground-state wave function from this study of GWB[8] is $\psi_1(1,0)=0.481(2s_{1/2})^2+0.864(2s_{1/2}1d_{3/2})+0.138(1d_{3/2})^2$ and that for the second 1^+ level at 0.709 MeV is $\psi_2(1,0)=-0.876(2s_{1/2})^2+0.471\times(2s_{1/2}1d_{3/2})+0.100(1d_{3/2})^2$. The theoretical energies for these levels are very close to the experimental values. The predicted energies for the $T=0$, 2^+, and 3^+ levels, however, are 2.7 and 2.9 MeV, respectively, instead of the 1.453 and 1.974 MeV for the levels studied in this experiment. A 2^+ and a 3^+ level have been observed in P^{30} nearer the predicted energies; it is possible that these states are more closely related to the wave functions of this simplified theory, which are $\psi_1(2,0)=1.0(2s_{1/2}1d_{3/2})$ and $\psi_1(3,0)=1.0(1d_{3/2})^2$.

In making matrix-element calculations to compare with the present experimental results, first the above approximate wave functions will be assumed for the levels involved in the transition studies. Secondly, a two-particle $2s_{1/2}1d_{5/2}$ configuration will be tried for the 1.453-MeV 2^+ level and 1.974-MeV 3^+ level; this is perhaps a reasonable second choice as it represents a simple excitation of the assumed core which could be at lower energies. The results of these calculations are summarized in Table II. All of the $B(M1)$ values are given in units of $\mu_N{}^2$. The experimental $B(E2)$ values are in units of e^2F^4, while the theoretical values are given in units of $(1+2\epsilon/e)^2e^2F^4$. The effective neutron charge and the effective proton charge are defined by ϵ and $e+\epsilon$, respectively, where ϵ represents the portion of the effective charge due to the quadrupole polarization of the core.

In the calculation of the theoretical $B(E2)$ values listed in Table II, the expectation values of the square of the nuclear radius $\langle r^2\rangle$ were obtained from harmonic-oscillator wave functions. The harmonic-oscillator parameter was chosen by comparing experimentally measured[18] R_{rms} for the closed core with that calculated for particles filling the appropriate harmonic-oscillator shells. It is interesting to point out that the value of $\langle r^2\rangle$ determined by a flat radial wave function, that is, $\frac{3}{5}(r_0A^{1/3})^2$, is about 26% smaller than the harmonic-oscillator values.

When assuming the $s_{1/2}d_{5/2}$ configuration for the 1.453-MeV level, the $B(M1)$ for the 1.453-MeV $2^+\to1^+$ ground-state transition is retarded by a factor of 8.3 and the $B(E2)$ implies an $\epsilon=2.5e$. On the other hand, when assuming the $s_{1/2}d_{3/2}$ configuration for the 1.453-MeV level, the $B(M1)$ for the same transition is retarded by a factor of 12.5 and the $B(E2)$ leads to an $\epsilon=0.07e$. While both configurations lead to $B(M1)$ values within an order of mag-

TABLE II. Experimental reduced transition probabilties compared with theoretical reduced transition probabilities that were calculated for the various listed initial-state configurations and for final-state wave functions given by Ref. 8. The theoretical $B(E2)$ values are given in units of $(1+2\epsilon/e)^2e^2F^4$ where the effective neutron charge and effective proton charge are given by ϵ and $e+\epsilon$, respectively.

Transition (MeV)	$J_i\to J_f$	Multipole	Experimental value	Initial state	Theoretical value
1.453→ 0	$2^+\to1^+$	$M1$	$1.4\times10^{-3}\mu_N{}^2$	$s_{1/2}d_{5/2}$	$1.2\times10^{-2}\mu_N{}^2$
				$s_{1/2}d_{3/2}$	$1.9\times10^{-2}\mu_N{}^2$
1.453→ 0	$2^+\to1^+$	$E2$	$0.45\ e^2F^4$	$s_{1/2}d_{5/2}$	$9.4\times10^{-3}(1+2\epsilon/e)^2e^2F^4$
				$s_{1/2}d_{3/2}$	$5.7\times10^{-2}(1+2\epsilon/e)^2e^2F^4$
1.974→ 0	$3^+\to1^+$	$E2$	$1.7\ e^2F^4$	$s_{1/2}d_{5/2}$	$0.60(1+2\epsilon/e)^2e^2F^4$
				$d_{3/2}{}^2$	$0.46(1+2\epsilon/e)^2e^2F^4$
1.974→ 0.709	$3^+\to1^+$	$E2$	$22\ e^2F^4$	$s_{1/2}d_{5/2}$	$0.85(1+2\epsilon/e)^2e^2F^4$
				$d_{3/2}{}^2$	$0.26(1+2\epsilon/e)^2e^2F^4$

nitude of the expected results, an $\epsilon = 2.5e$ implies a larger collective enhancement than expected in the mass region; this suggests that $s_{1/2}d_{3/2}$ is the more favored configuration of the two considered for the 1.453-MeV state.

When assuming either the $d_{3/2}{}^2$ or $s_{1/2}d_{5/2}$ configuration for the 1.974-MeV level the $B(E2)$ values for the 1.974-MeV $3^+ \rightarrow 1^+$ ground-state branch yield an $\epsilon = 0.3e$. The $B(E2)$ for the 1.974-MeV $\rightarrow$ 0.709-MeV $3^+ \rightarrow 1^+$ branch implies an unreasonably large $\epsilon = 3.5e$ when using the $d_{3/2}{}^2$ configuration for the 1.974-MeV level. The $B(E2)$ for the same transition when using the $s_{1/2}d_{5/2}$ configuration leads to an $\epsilon = 1.7e$, which although somewhat larger than expected is nevertheless significantly less than an $\epsilon = 3.5e$. Hence, for the 1.974-MeV state $s_{1/2}d_{5/2}$ would appear to be the more favored configuration of the two considered. The large experimental $B(E2)$ for the 0.709-MeV branch could be related to some form of collective enhancement.

The large shell-model calculation[9] including the addition of the $1d_{5/2}$ and $1f_{7/2}$ shells, which is presently under study for the $A = 30$ region, is expected to yield more accurate wave functions for P^{30}. As part of this large calculation Wildenthal *et al.*[19] have already made preliminary shell-model calculations for P^{30} assuming an inert O^{16} core and two-particle interactions for the outer nucleons in the $2s_{1/2}$, $1d_{3/2}$, and $1d_{5/2}$ shells where up to two $1d_{5/2}$ holes are allowed. The results which reflect the inclusion of only the $1d_{5/2}$ shell in addition to the $1d_{3/2}$ and $2s_{1/2}$ shells predict theoretical energy levels in P^{30} which are in much closer agreement with the observed energies than are the levels calculated[8] with a closed Si^{28} core. Better agreement is also expected in a comparison of the electromagnetic transition probabilities for P^{30} with those calculated from the complete wave functions. Any large discrepancies in such a comparison will indicate the need for additional theoretical approaches.

---

†Work supported in part by the National Science Foundation.

[1]P. M. Endt and C. H. Paris, Phys. Rev. 110, 89 (1958).

[2]C. Van der Leun and P. M. Endt, Phys. Rev. 110, 96 (1958).

[3]P. M. Endt and C. Van der Leun, Nucl. Phys. 34, 1 (1962).

[4]E. E. Baart, L. L. Green, and J. C. Willmott, Proc. Phys. Soc. (London) 79, 237 (1962).

[5]R. A. Moore, Ph. D. thesis, University of Kansas, 1963 (unpublished).

[6]G. I. Harris and A. K. Hyder, Jr., Phys. Letters 22, 159 (1966); G. I. Harris and A. K. Hyder, Jr., Phys. Rev. 157, 958 (1967); G. I. Harris, A. K. Hyder, and J. Walinga, *ibid.* 187, 1413 (1969).

[7]C. W. Vermette, W. C. Olsen, D. A. Hutcheon, and D. H. Sykes, Nucl. Phys. A111, 39 (1968).

[8]P. W. M. Glaudemans, G. Wiechers, and P. J. Brussard, Nucl. Phys. 56, 529,548 (1964).

[9]J. B. McGrory, private communication.

[10]S. H. Henson, S. Cochavi, M. Marmor, J. M. McDonald, and D. B. Fossan, Bull. Am. Phys. Soc. 14, 628 (1968).

[11]E. F. Kennedy, D. H. Youngblood, and A. E. Blaugrund, Phys. Rev. 158, 897 (1967).

[12]R. E. Pixley and A. R. Poletti, Bull. Am. Phys. Soc. 14, 125 (1969).

[13]A. N. James, J. F. Sharpey-Schafer, P. R. Alderson, D. C. Bailey, J. L. Durell, and M. W. Greene, in *Proceedings of the International Conference on Properties of Nuclear States, Montréal, Canada, 1969,* edited by M. Harvey *et al.* (Presses de l'Université de Montréal, Montréal, Canada, 1969), p. 113.

[14]K. W. Jones, A. Z. Schwarzschild, E. K. Warburton, and D. B. Fossan, Phys. Rev. 178, 1773 (1969).

[15]M. L. Roush, M. A. Wilson, and W. F. Hornyak, Nucl. Instr. Methods 31, 112 (1964).

[16]C. Broude, P. J. M. Smulders, and T. K. Alexander, Nucl. Phys. A90, 321 (1967).

[17]G. Morpurgo, Phys. Rev. 110, 721 (1958).

[18]H. R. Collard, L. R. B. Elton, and R. Hofstadter, in *Landolt-Börnstein Numerical Data and Functional Relationships in Science and Technology,* edited by K.-H. Hellwege and H. Schopper (Springer-Verlag, Berlin, Germany, 1967), New Series, Group I, Vol. 2.

[19]B. H. Wildenthal, J. B. McGrory, E. C. Halbert, and P. W. M. Glaudemans, Phys. Letters 27B, 611 (1968).